

RESEARCH

Open Access



Transcriptomic and physiological insights into auxin-mediated root growth and potassium uptake in tobacco under low-potassium stress

Kunhao Guan¹, Yingying Li¹, Yuyin Zhang¹, Jie Yang¹, Zixuan Ge¹ and Xiaoyan Dai^{1*}

Abstract

Background Improving potassium uptake efficiency in plants is crucial for agricultural production. Auxin is a key plant hormone that promotes root growth and enhances the ability of plants to absorb and accumulate mineral nutrients. To investigate the role of auxins in root growth and potassium uptake mechanisms under low-potassium stress, we used tobacco as a model plant and conducted hydroponic experiments.

Results Low-potassium stress significantly impairs root development and potassium uptake in tobacco plants. Under these conditions, exogenous Indole acetic acid (IAA) enhanced root development and increased potassium uptake, whereas N-1-naphthylphthalamic acid (NPA) inhibited root growth and adversely affected potassium absorption and retention. Transcriptome sequencing under low-potassium conditions identified 8,381 differentially expressed genes (DEGs) between the two different treatment groups that were primarily enriched in pathways related to photosynthesis-antenna proteins, photosynthesis, plant hormone signal transduction, and the MAPK signaling pathway. Analysis of the DEGs associated with auxin signaling, potassium ion channels, transporters, and transcription factors revealed several key genes involved in low-potassium stress response, including *KUP6*, *IAA14*, *ARF16*, *PIN1*, *SKOR*, *NPF7.3*, and *AP2/ERF*. Notably, *KUP6* was upregulated following IAA treatment and downregulated by NPA, indicating that this potassium ion transporter gene plays a crucial role in the auxin-mediated alleviation of low potassium stress in tobacco, which is likely linked to endogenous auxin levels.

Conclusions Our study revealed that potassium deficiency impairs root development and uptake in tobacco and that auxin is critical in mitigating this stress. This study highlights the regulatory function of auxin in enhancing root growth and potassium absorption under low potassium conditions, offering insights into the molecular mechanisms of potassium stress response.

Keywords Auxin, Low potassium, Root growth, Potassium uptake, Transcriptome

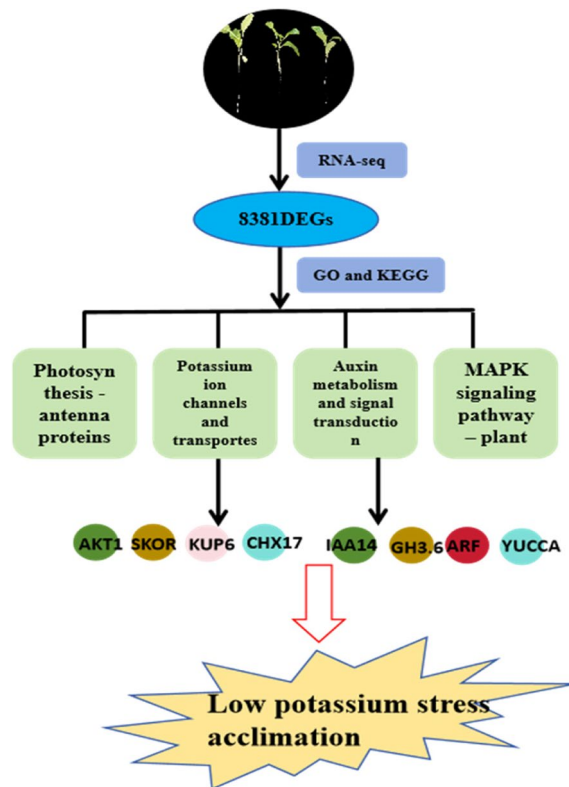
*Correspondence:

Xiaoyan Dai
daixiaoy319@163.com



© The Author(s) 2025. **Open Access** This article is licensed under a Creative Commons Attribution-NonCommercial-NoDerivatives 4.0 International License, which permits any non-commercial use, sharing, distribution and reproduction in any medium or format, as long as you give appropriate credit to the original author(s) and the source, provide a link to the Creative Commons licence, and indicate if you modified the licensed material. You do not have permission under this licence to share adapted material derived from this article or parts of it. The images or other third party material in this article are included in the article's Creative Commons licence, unless indicated otherwise in a credit line to the material. If material is not included in the article's Creative Commons licence and your intended use is not permitted by statutory regulation or exceeds the permitted use, you will need to obtain permission directly from the copyright holder. To view a copy of this licence, visit <http://creativecommons.org/licenses/by-nc-nd/4.0/>.

Graphical Abstract



Introduction

Potassium is one of the most abundant cations in plant cells [1], comprising 2–10% of the plant dry weight [2]. It plays a crucial role in physiological processes such as osmoregulation, charge balance, and enzyme activation [3–6], and has earned the title “quality and stress resistance element” in plants. Despite potassium ion concentration in soil typically ranging 0.025–5 mmol/L [7], the rhizosphere concentration often decreases to <0.3 mmol/L [8], leading to low-potassium stress in several crop types.

In response to low-potassium stress, plants activate high-affinity potassium uptake systems and regulate potassium channel transport [9–11]. Simultaneously, they adjust their physiological and morphological characteristics, particularly in the root system, which is highly sensitive to potassium deficiency signals [6, 12, 13]. Under such stress, root growth slows, total root length and volume decrease substantially, and biomass distribution shifts between the aboveground and belowground parts [14, 15]. In contrast, low-potassium-tolerant plants develop more extensive root systems with enhanced

primary root growth, lateral root formation, and root hair elongation. These adaptations increase root surface area, thus facilitating better potassium absorption from the soil [16–18].

Auxin, an endogenous plant hormone [19], is primarily produced in young tissues and is transported to target sites through polar transport. This hormone promotes root growth and enhances the ability of plants to absorb and accumulate mineral nutrients [20]. Transcriptome analyses of rice, maize, and wheat roots under low-potassium conditions have identified numerous auxin-related genes [21–23]. Further studies have shown that the potassium ion channel *AKT1* regulates auxin redistribution by influencing *PIN1*, thereby affecting root growth [24]. In addition, the potassium transporter *TRHI* is an integral part of the auxin transport system in Arabidopsis roots [25]. The auxin response factor *ARF2* also plays a significant role in the response of plants to external potassium supply by regulating the transcription of *HAK5* [26]. Low-potassium stress has been shown to induce ethylene production, which promotes the transcription of central cylinder auxin transport genes, such

as *PIN3* and *PIN7*, thereby further influencing auxin distribution in roots [27]. These findings indicate that auxin is crucial for root formation and potassium uptake during potassium deficiency.

Exogenous indole-3-acetic acid (IAA) can enhance plant stress resistance and mitigate nutrient stress [28–31]. The synthetic compound N-1-naphthylphthalamic acid (NPA) inhibits auxin transport by binding to the auxin efflux carrier PIN and is widely used in auxin-related research [32]. Our previous study on tobacco showed that adding appropriate concentrations of exogenous auxin improved root growth, enhanced potassium uptake capacity and affinity, and increased overall plant potassium concentration. However, the extent to which the physiological and morphological responses of tobacco under low-potassium stress are tied to changes in endogenous auxin and the precise mechanisms through which auxin regulates potassium uptake in tobacco roots remain unclear. The aim of this study is to understand the regulatory role of auxins in root growth and potassium uptake under low-potassium stress using tobacco as a model to investigate these mechanisms through transcriptome sequencing and physiological experiments.

Methods

Plant materials

The plant material used in this study was the tobacco variety K326, and the experiment was conducted at the Key Laboratory of Tobacco Cultivation at Henan Agricultural University, Zhengzhou, China. Tobacco seeds were germinated and sown in sponges moistened with distilled water. After reaching the small cross stage, the seedlings were uniformly transplanted into black containers filled with Hoagland's nutrient solution and perlite and grown in a growth chamber under the following conditions: day temperature, 28 ± 2 °C; night temperature, 18 ± 2 °C; 14 h photoperiod; 4000 lx light intensity; and relative humidity, 65–70%, as described in a previous study [15]. When tobacco seedlings developed three to four true leaves, seedlings with uniform growth were selected, and their roots were washed with distilled water and transplanted into hydroponic boxes. Initially, the seedlings were placed in potassium-free Hoagland's nutrient solution for 48 h to induce potassium starvation, followed by cultivation in nutrient solutions with potassium concentrations of 0.15 mmol/L (low potassium level) and 5 mmol/L (normal potassium level) [33]. During cultivation, the nutrient solution was aerated daily for 4 h and replaced every 4 d to maintain stable nutrient concentrations. After 8 d of treatment with different potassium levels, 10 μ mol/L of auxin, 40 μ mol/L of auxin inhibitor, and a 4 d pretreatment without added hormone (IAA and NPA concentrations obtained from the pre-experiment), samples were

collected. Relevant indexes were measured, and each treatment was repeated in triplicate.

Root dry weight and scanning index determination

Tobacco roots were cut and placed in a paper bag of known weight and placed in the oven at 100–105 °C for 30 min to dry the roots, then the oven temperature was lowered to approximately 65 °C, baked until constant weight, removed and dry weight was calculated following the methods described by [34]. Tobacco roots were cut to ensure their integrity, and the complete root system was scanned using a digital scanner (EPSON Expression1000XL, Seiko, Japan). Next, sample roots were quantitatively analyzed using the WinRHIZO Root Analysis System software for seven indices of the root system: total root length, root volume, total surface area of the root, root projected area, average diameter of the root, number of root tips, and number of root bifurcations.

Determination of root physiological indexes in tobacco plants

Root activity was measured using the 2,3,5-triphenyltetrazolium chloride TTC method [35]. The fresh samples were collected for immediate testing. Root H⁺-ATPase activity was measured according to the manufacturer's instructions (kit purchased from Nanjing Jiancheng Bioengineering Institute). Soluble protein content in the roots was determined using the Coomassie Brilliant Blue G-250 colorimetric method [36].

Determination of endogenous growth hormone concentration in the root system

Fresh tobacco root samples (0.5 g) were collected from the primary root tip (0–2 cm) and the lateral root zone (4–8 cm). Samples were snap-frozen in liquid nitrogen and stored at –80 °C. To determine auxin concentration, the samples were ground into a homogenate in an ice bath with 3–5 mL of 80% methanol extraction solution and extracted at 4 °C for 4 h. The samples were then centrifuged at 1000 rpm for 15 min and the supernatant was collected for indirect enzyme-linked immunosorbent assay [37].

Determination of potassium content and uptake kinetics in roots

Approximately 0.1 g of dried and ground samples was accurately weighed and passed through a 0.2 mm mesh sieve. We used 1 mmol/L HCl and a flame photometer [33] to measure the potassium content in the roots using the depletion method as previously described [15]. After cultivation, the test seedlings were treated with for 2 d in a potassium-free solution, with the starvation solution being changed daily. The depletion experiment was

conducted by placing the seedlings in a black conical flask containing 50 mL of the depletion solution (composed of 0.4 mmol/L KNO₃ and 0.2 mmol/L CaSO₄). Samples were collected every 4 h until the potassium concentration in the depletion solution approached zero. After each sampling, the samples were replenished with 10 mL of deionized water. The potassium concentration in the depletion solution was measured using a flame photometer. The potassium ion depletion curve was plotted using the potassium concentration of the depletion solution as the ordinate and depletion time as the abscissa. The quadratic equation model was $Y = a + bX + cX^2$, where X represents absorption time and Y represents potassium concentration in the depletion solution at a specific time. Using the relevant equation, we calculated Vmax and Km for potassium ion absorption by the roots [38], reflecting the potassium absorption characteristics of the roots.

Determination of potassium ion flow using a non-invasive microtest

When the tobacco seedlings completed their initial growth phase, potassium starvation was applied for 3 and 5 d. After treatment, tobacco seedlings with uniform growth in each group were selected, and the tobacco root system, approximately 0–3 cm from the root tip, was gently cut with sterilized experimental scissors and placed into a disc containing distilled water for testing and observation [39]. The non-invasive microtest (NMT) technology was provided by the Beijing Xuyue Company.

RNA isolation and library preparation

Root tissues from each of the hormone-treated and control samples in the low-potassium state were collected for mRNA sequencing in triplicate. Total RNA was extracted using the TRIzol reagent (Invitrogen, Carlsbad, CA, USA) according to the manufacturer's protocol. RNA purity and quantity were evaluated using a NanoDrop 2000 spectrophotometer (Thermo Fisher Scientific, USA). RNA integrity was assessed using the Agilent 2100 Bioanalyzer (Agilent Technologies, Santa Clara, CA, USA). Libraries were constructed using the VAHTS Universal V6 RNA-seq Library Prep Kit (Vazyme Biotech, China), according to the manufacturer's instructions. Transcriptome sequencing and analysis were performed by OE Biotech Co., Ltd. (Shanghai, China).

RNA sequencing and differentially expressed gene analysis

The libraries were sequenced on an Illumina NovaSeq 6000 platform, generating 150 bp paired-end reads. About 47.83 M raw reads for each sample were generated. Raw reads in fastq format were initially processed using fastp [40], where low-quality reads were removed to obtain clean reads. About 46.97 clean reads for each

sample were retained for subsequent analyses. Clean reads were mapped to the reference genome using HISAT2 [41]. FPKM [42] of each gene was calculated and the read counts of each gene were obtained by HTSeq-count [43]. Differential expression analysis was performed using DESeq2. A Q value < 0.05, fold change > 2, or fold change < 0.5 was set as the threshold for significantly differentially expressed gene (DEG). Subsequently, Gene Ontology (GO) GO [44] and KEGG [45] pathway enrichment analyses of DEGs were conducted based on the hypergeometric distribution algorithm to screen items with significant enrichment functions.

Quantitative reverse transcription-polymerase chain reaction analysis

In order to verify the expression patterns of the identified DEGs, we performed quantitative reverse transcription-polymerase chain reaction (qRT-PCR) analysis. RNA was extracted using a kit from Nanjing Novozymes Biologicals, reverse transcribed into cDNA using a kit (ABM, Canada), and the relative expression of the genes was analyzed using real-time qRT-PCR with SYBR Green PCR Master mix in an IQ5 photocycling system. NtActin was used as an internal reference gene and the relative expression of the gene was calculated using the $2^{-\Delta\Delta Ct}$ method. The primer sequences are shown in Table 1. Three biological replicates were used in the experiment and the results were expressed as mean \pm standard deviation (SD).

Table 1 Primer sequences for qRT-PCR

| Gene | Primers |
|--------------|---|
| AB196790 | 5'-CTGAGGAGAATGTGGAAATAGT-3' 5'-AAAGCTCCTTTATCTCTTCGTG-3' |
| AB196791 | 5'-CACTATTGTCATGGCGGATG-3' 5'-TCTTCGGTACATCCGTTTCTG-3' |
| AB196792 | 5'-AGTGAAACAACCTTGAGAGTACCTC-3' 5'-GAGAAGCATAAAGCTACAGTGG-3' |
| AB353341 | 5'-TCTGTTCTACCATCACAACT-3' 5'-ACATGGAGTAGGTGTATCCTT-3' |
| DQ841950 | 5'-CAGGCATGGCGTTTATACT-3' 5'-CCGCGACAATTCCTTCTC-3' |
| XM_016638787 | 5'-GCTAGTGTATGTCAGTGGATG-3' 5'-TCAAACCATGTATGTCATCCCC-3' |
| AB158612 | 5'-AACAGTTTGGTTGGAGTCTGG-3' 5'-CATGAAGATTAAGGCGGAGTG-3' |

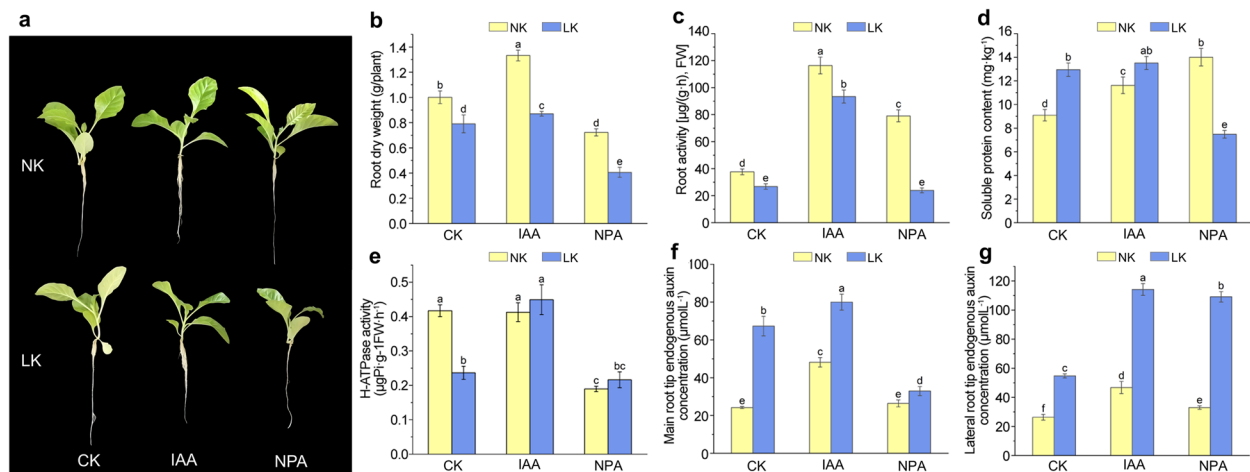


Fig. 1 Effects of Exogenous Auxins and Inhibitors on the Root System of Tobacco Plants Under Normal and Low Potassium Levels. **a** Morphological Changes in Tobacco Seedlings. **b** Dry Weight of Plant Roots. **c** Root Viability. **d** Soluble Proteins. **e** H-ATPase Content. **f** Auxin Concentration in the Main Root Tip. **g** Auxin Concentration in the Lateral Root Tip. The bars represent the averages \pm standard deviations of three replicates. Different letters above the bars indicate significant differences between treatments at $P < 0.05$. NK: normal potassium; LK: low potassium; CK: untreated control; IAA: indole acetic acid; NPA: naphthylphthalamic acid

Results

Effects of auxin treatment on root growth under low potassium stress

To investigate the effects of exogenous IAA and NPA on root growth under low-potassium stress, we examined the morphological and physiological characteristics of tobacco roots, as well as the accumulation of endogenous auxin under different treatments. Low potassium stress causes slower root growth and symptoms such as leaf yellowing and wilting. Treatment with exogenous IAA alleviated these symptoms, whereas treatment with NPA

exacerbated them (Fig. 1a). Consistent with these findings, the root dry matter accumulation was found to be higher under normal potassium conditions than under low-potassium conditions. Specifically, IAA treatment increased dry matter accumulation by 33.15% and 10.12% under normal and low-potassium conditions, respectively, whereas NPA treatment reduced dry matter accumulation by 27.79% and 48.67%, respectively (Fig. 1b). These trends in root morphology parameters confirmed that auxin promotes root growth under low potassium stress (Table 2).

Table 2 Root scan characteristics

| Root index | K level | Treatment | | |
|--------------------|---------|----------------------|---------------------|---------------------|
| | | 0 | IAA | NPA |
| Length | N | 906.96 \pm 30.70a | 851.03 \pm 13.60b | 533.53 \pm 18.06c |
| | L | 409.70 \pm 35.78 d | 513.07 \pm 21.42c | 292.64 \pm 25.56e |
| Volume | N | 1.19 \pm 0.08a | 1.37 \pm 0.09a | 0.43 \pm 0.03 d |
| | L | 0.66 \pm 0.02c | 0.85 \pm 0.02b | 0.58 \pm 0.02 cd |
| Surface area | N | 122.66 \pm 6.02a | 112.34 \pm 5.32b | 105.74 \pm 5.19c |
| | L | 48.19 \pm 2.74 d | 50.19 \pm 2.89 d | 40.16 \pm 2.29e |
| Projection area | N | 37.49 \pm 2.00a | 35.64 \pm 1.37b | 33.17 \pm 1.74c |
| | L | 15.11 \pm 1.46e | 16.13 \pm 0.57 d | 13.74 \pm 1.33f |
| Diameter | N | 0.40 \pm 0.03a | 0.43 \pm 0.02a | 0.32 \pm 0.03c |
| | L | 0.39 \pm 0.01a | 0.33 \pm 0.00c | 0.38 \pm 0.01b |
| Root tip number | N | 1615 \pm 27a | 1506 \pm 54b | 1324 \pm 20c |
| | L | 464 \pm 22e | 830 \pm 70 d | 440 \pm 21e |
| Bifurcation number | N | 5461 \pm 163a | 5631 \pm 256a | 2116 \pm 63c |
| | L | 2543 \pm 90b | 1970 \pm 60c | 2002 \pm 71c |

N (5 mmol/L); L (0.15 mmol/L); different lowercase letters following the numbers in the same row indicate significant differences ($P < 0.05$)

Root physiological indicators reflect the overall growth and development of the roots. We measured root vitality (Fig. 1c), soluble protein content (Fig. 1d), and ATPase activity (Fig. 1e) at different potassium levels. Root vitality decreased by 28.90% under low-potassium conditions compared to normal potassium levels without treatment. However, IAA treatment significantly enhanced root vitality, with a 2.5-fold increase under low-potassium conditions compared to that in untreated plants. The soluble protein content significantly increased with both IAA and NPA treatments under normal potassium levels. Under the low-potassium conditions, IAA treatment slightly increased the soluble protein content compared to the untreated controls, although the difference was not significant. However, NPA treatment significantly reduced soluble protein content. Furthermore, ATPase activity in roots treated with IAA under low-potassium conditions was 89.86% higher than that in untreated plants. These results suggest that auxin enhances the metabolic capacity of tobacco roots under low-potassium stress, whereas auxin inhibitor addition reduces this stimulatory effect.

We also examined changes in endogenous auxin levels in plant roots treated with exogenous IAA and NPA under different potassium conditions (Fig. 1f and g). Without any treatment, auxin concentrations in the primary and lateral root tips under low-potassium conditions were significantly higher than those under the normal potassium conditions. After exogenous IAA application, the auxin content in the primary root tips significantly increased under both potassium conditions compared to the untreated controls. Conversely, NPA treatment decreased the auxin concentrations in primary root tips by up to 49% under low-potassium conditions. Interestingly, in both the IAA and NPA treatments, auxin concentrations in the lateral root tips increased significantly compared with those in the untreated controls. Specifically, IAA treatment increased auxin concentrations in the lateral root tips under low-potassium conditions to 1.72 times that of untreated plants, whereas NPA treatment led to an increase of 1.55 times under similar conditions. Auxin concentrations in the lateral root tips under both potassium conditions were significantly lower than those in the corresponding IAA-treated plants.

Effects of auxin treatment on potassium uptake under low potassium stress

To examine potassium ion absorption capacity differences under various treatments, we used NMT to monitor potassium ion flux and velocity in the plant roots in real time.

Under normal potassium conditions, potassium efflux was observed in the roots, regardless of whether the plants were starved for three or five days. Exogenous IAA treatment further increased this efflux, particularly in the 5-day starvation group, in which a 352% increase was observed (Fig. 2a). In contrast, the increase in the 3-day group was less pronounced (Fig. 2b). NPA, an inhibitor of polar auxin transport, also enhanced efflux but to a lesser extent. Under the low-potassium conditions, roots exhibited significant potassium influx after three or five days of starvation. IAA treatment further increased potassium influx by 63% in the 3-day group and 105% in the 5-day group compared to the untreated controls. In contrast, NPA reduced potassium uptake in both groups, with more pronounced inhibition in the 5-day group ($p < 0.05$).

Kinetic parameters such as V_{max} and K_m were used to quantify the potassium uptake characteristics. By analyzing the relationship between the potassium concentration in the depletion solution and time, we calculated V_{max} and K_m for each treatment. Significant differences were observed in these parameters across treatments. Under the low-potassium conditions, IAA treatment significantly increased V_{max} and decreased K_m , indicating enhanced potassium affinity in the roots. Conversely, NPA treatment decreased V_{max} and increased K_m , thereby reducing potassium uptake efficiency (Table 3).

In addition, potassium ion accumulation in the roots was measured across treatments (Fig. 2c). The potassium content in the roots under low-potassium stress was significantly lower than that under normal conditions. IAA treatment increased potassium content by 2.43-fold compared with untreated low-potassium plants, whereas NPA-treated plants showed no significant difference from untreated controls.

Transcriptome sequencing and quality assessment

To further elucidate the molecular mechanisms by which IAA and NPA regulate root growth and potassium absorption under low-potassium stress, we performed RNA-seq analysis on all samples from the different treatments and controls under low-potassium conditions. After removing reads containing adapters and low-quality data, we obtained a total of 62.75 G of clean data. The effective data for each sample ranging from 6.90 to 7.07 G, with Q30 base distributions between 96.75% and 97.13%, and an average GC content of 44.28%. Clean reads were aligned to the specified reference genome using Hisat2, with alignment rates ranging from 78.81 to 82.32% (Table 4), indicating a good sequencing quality.

We used FPKM values to compare gene expression levels among different samples and conducted further

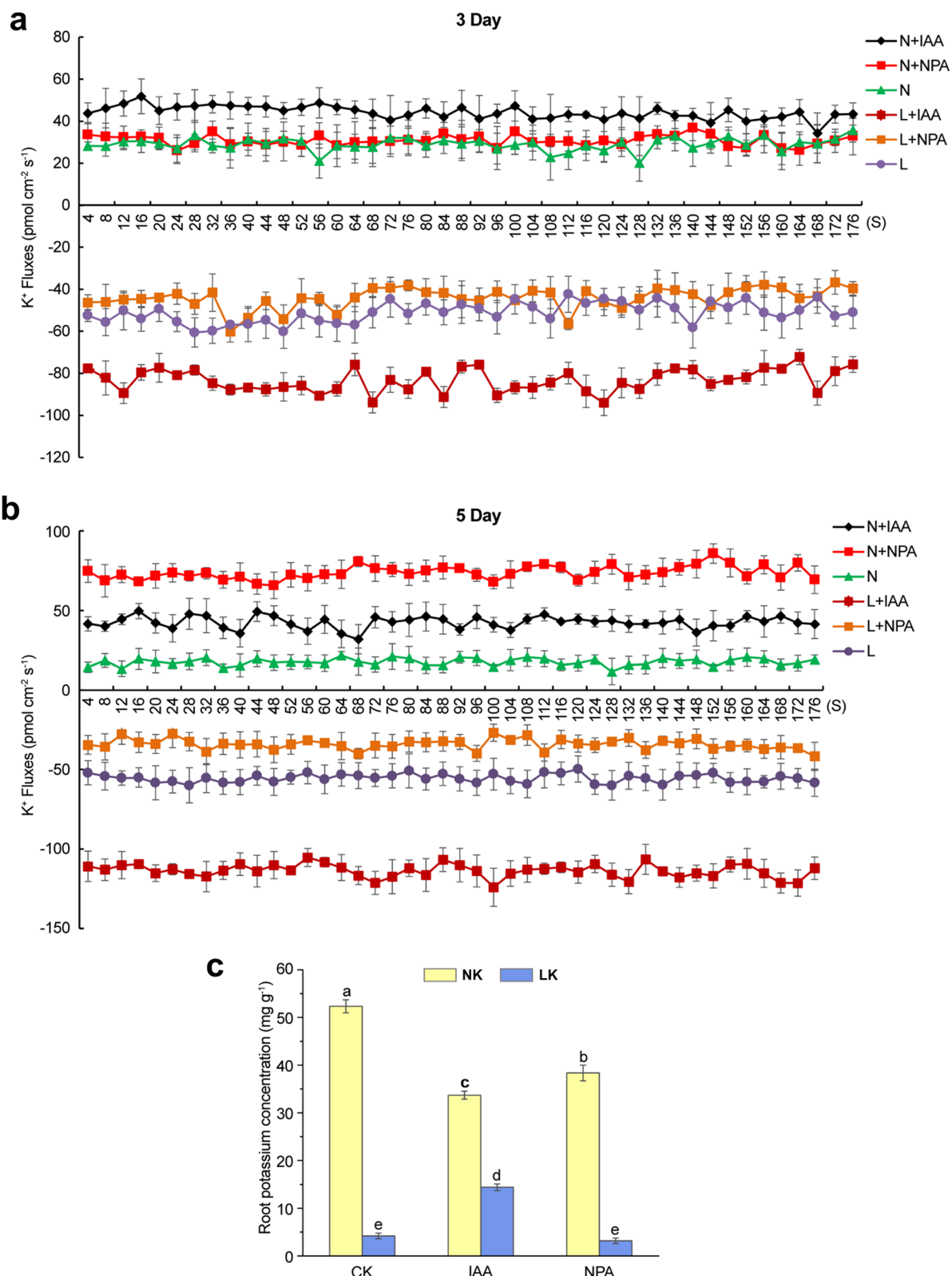


Fig. 2 Effects of exogenous auxins and inhibitors on potassium uptake in tobacco plants under normal and low potassium levels. **a** Potassium ion flux after 3 d of starvation. **b** Potassium ion flux after 5 d of starvation. **c** Potassium ion content in the roots. Bars represent the averages \pm SD of three replicates. Different letters above the bars indicate significant differences between treatments at $P < 0.05$. NK: normal potassium; LK: low potassium; CK: untreated control IAA: indole acetic acid; NPA: naphthylphthalamic acid

Table 3 Difference of kinetics of potassium absorption in plant roots

| Potassium level (mmolL ⁻¹) | Treatment | Vmax (μmolg ⁻¹ FW h ⁻¹) | Km (μmolL ⁻¹) |
|--|-----------|--|---------------------------|
| 5 | 0 | 24.32b | 0.0044b |
| | IAA | 49.71a | 0.0051ab |
| | NPA | 20.27b | 0.0060a |
| 0.15 | 0 | 2.64b | 2.15E-05a |
| | IAA | 5.15a | 1.23E-05c |
| | NPA | 2.98b | 1.54E-05b |

Different lowercase letters following the numbers in the same row indicate significant differences ($P < 0.05$)

detailed analysis, revealing significant statistical correlations among biological replicates, with Pearson correlation coefficients exceeding 0.85 (Fig. 3a). In addition, PCA effectively distinguished between the different treatment groups (Fig. 3b), indicating that the gene expression profiles in the treated tobacco plants changed significantly under low potassium stress.

DEG screening and clustering analysis

We screened the DEGs between the treatment groups using a threshold of $|\log_2(\text{fold change})| > 1$ and $\text{padj} < 0.05$. In the samples treated with exogenous IAA, 7,200 DEGs were identified, with 4,176 upregulated and 3,024 downregulated genes. In the NPA-treated samples, 2,646 DEGs were identified, including 1,511 upregulated and 1,135 downregulated genes (Fig. 4a). A comparison

between the exogenous IAA- and NPA-treated samples revealed 1,465 overlapping DEGs (Fig. 4b). Volcano plots were used to visualize the statistical significance of padj and fold changes, facilitating the identification of genes with substantial changes (Fig. 4c and d).

GO and KEGG pathway analysis

GO analysis was performed to categorize the DEGs into biological processes (BP), cellular components (CC), and molecular functions (MF). In the CK vs. IAA comparison (Fig. 5a), 4,985 DEGs were enriched in 199 functional subclasses. The most prominent GO terms in the BP were GO:0006952 (defense response, 232 DEGs), GO:0010200 (response to chitin, 114 DEGs), and GO:0009873 (ethylene-activated signaling pathway, 122 DEGs). In CC, the most common term was GO:0005576 (extracellular region, 314 DEGs), whereas in MF, the most prevalent terms were GO:0003700 (DNA-binding transcription factor (TF) activity, 571 DEGs) and GO:0043565 (sequence-specific DNA binding, 326 DEGs). In the CK vs. NPA comparison (Fig. 5b), 1,911 DEGs were enriched in 168 functional subclasses. The most frequent BP terms were GO:0006952 (defense response, 127 DEGs), GO:0010200 (response to chitin, 86 DEGs), and GO:0009873 (ethylene-activated signaling pathway, 77 DEGs). In CC, GO:0046872 (metal ion binding, 342 DEGs) was the most common, whereas in MF, GO:0003700 (DNA-binding TF activity, 254 DEGs) and GO:0043565 (sequence-specific DNA binding, 133 DEGs) were the most common. These results indicated

Table 4 Summary of RNA-seq

| Sample | Clean reads | Q30 (%) | GC content (%) | Total mapped reads (Percentage in clean reads) | Multiple mapped reads (Percentage in clean reads) | Uniquely mapped reads (Percentage in clean reads) |
|--------|-------------|---------|----------------|--|---|---|
| CK_1 | 7.00 | 96.92 | 44.2 | 37,255,861 (78.81%) | 3,549,595 (7.51%) | 33,706,266 (71.30%) |
| CK_2 | 6.87 | 97.13 | 44.09 | 36,869,450 (79.48%) | 3,492,064 (7.53%) | 33,377,386 (71.95%) |
| CK_3 | 6.96 | 96.93 | 44.05 | 37,411,969 (79.77%) | 3,479,650 (7.42%) | 33,932,319 (72.35%) |
| IAA_1 | 7.07 | 96.83 | 43.65 | 37,987,758 (79.99%) | 3,413,495 (7.19%) | 34,574,263 (72.81%) |
| IAA_2 | 6.90 | 97.02 | 43.6 | 37,684,265 (81.13%) | 3,453,280 (7.43%) | 34,230,985 (73.70%) |
| IAA_3 | 7.03 | 96.75 | 43.56 | 38,921,122 (82.32%) | 3,505,116 (7.41%) | 35,416,006 (74.90%) |
| NPA_1 | 6.90 | 96.92 | 43.78 | 38,180,794 (82.07%) | 3,490,709 (7.50%) | 34,690,085 (74.57%) |
| NPA_2 | 7.05 | 96.77 | 43.76 | 38,810,712 (81.86%) | 3,488,603 (7.36%) | 35,322,109 (74.50%) |
| NPA_3 | 6.97 | 96.97 | 43.83 | 38,505,933 (81.92%) | 3,569,760 (7.59%) | 34,936,173 (74.33%) |

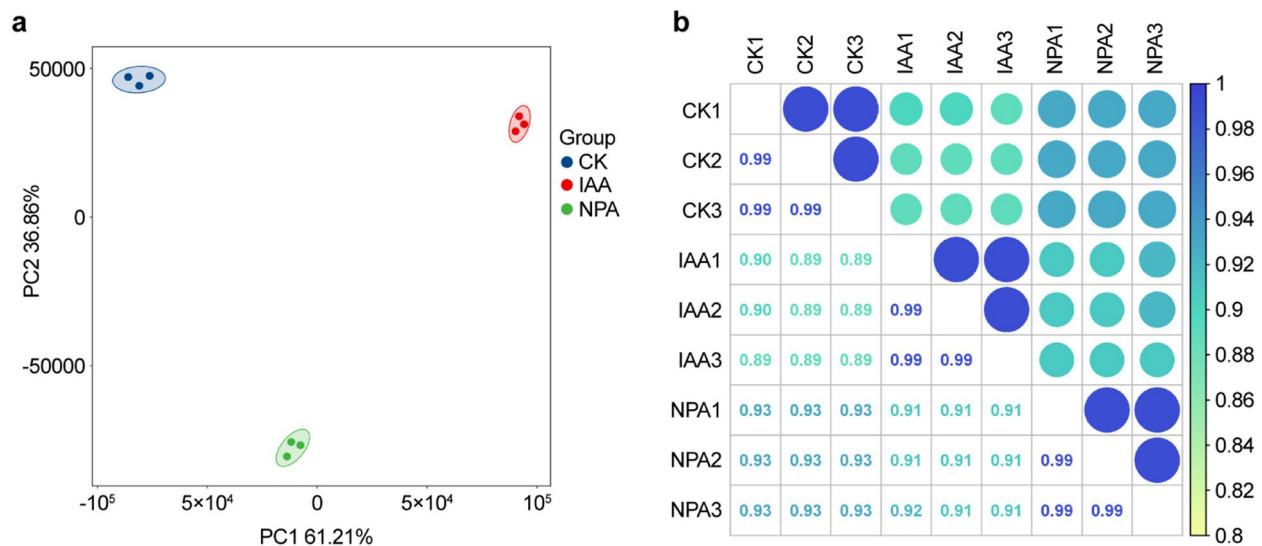


Fig. 3 A comprehensive transcriptome analysis. **a** Principal component analysis (PCA) of gene expression values across all samples. The axes represent principal components PC1 and PC2, explaining 98.07% of the variance. Each color represents a different treatment, with three biological replicates for each treatment, resulting in nine samples **b** Pearson's correlation coefficient analysis of gene expression values across all samples

similar functional classifications between the two treatments, although the number of DEGs varied between the categories.

KEGG database was used to analyze genomic and biochemical pathways. In total, 1,080 DEGs from the IAA treatment and 461 DEGs from the NPA treatment were enriched in 112 and 86 KEGG pathways, respectively. Pathways with a p-value < 0.05 were considered significantly enriched. The top 20 most enriched pathways in each comparison group were selected for further analysis. In the CK vs. IAA comparison (Fig. 5c), DEGs were enriched in pathways, including photosynthesis-antenna proteins, photosynthesis, phenylpropanoid biosynthesis, plant hormone signal transduction, the MAPK signaling pathway (in plant), starch and sucrose metabolism, and pentose and glucuronate interconversions. In the CK vs. NPA comparison (Fig. 5d), DEGs were enriched in photosynthesis-antenna proteins, Photosynthesis, Glutathione metabolism, the MAPK signaling pathway-plant, carbon fixation in photosynthetic organisms, sulfur metabolism, and plant hormone signal transduction. Notably, pathways such as photosynthesis-antenna proteins, Photosynthesis, and MAPK signaling pathways were enriched in both IAA and NPA treatments, suggesting that these pathways play critical roles in the response of tobacco seedlings to low-potassium stress during auxin treatment.

Auxin metabolism and signal transduction responses to exogenous IAA and NPA

We analyzed the expression levels of genes involved in auxin metabolism and signal transduction (Fig. 6). *YUCCA*,

a key enzyme in the endogenous IAA synthesis pathway, was significantly affected by the exogenous IAA and NPA treatments. *YUCCA3* and *YUCCA8* were upregulated in response to exogenous IAA, whereas *YUCCA9* was downregulated in NPA-treated samples, consistent with the changes in endogenous IAA levels. The *AUX/IAA*, *GH3*, and *SAUR* gene families, which are early key responders to auxin signaling, were also analyzed. Among the 38 identified gene family members, five showed significant expression in both treatment groups. Exogenous IAA significantly stimulated the expression of *IAA14* and *GH3.6*, while NPA inhibited their expression. The two *SAUR* genes exhibited reduced transcript levels after IAA and NPA treatments.

Auxin response factors (ARFs), which are critical regulators of the IAA signaling pathway, also display differential expression. *ARF8* and *ARF18* expression decreased in both treatment groups, whereas *ARF16* expression was significantly upregulated in the IAA-treated group. IAA enters plant cells through the *AUX1/LAX* family and is localized to the plasma membrane. In the present study, *LAX1* expression was upregulated in the IAA-treated group and downregulated in the NPA-treated group.

PIN proteins, the primary transporters of auxin efflux, are crucial for polar auxin transport. Our results showed that expression of *PIN1*, *PIN2*, and *PIN3* was upregulated in response to the exogenous IAA treatment.

Potassium absorption and transport-related DEGs response to exogenous IAA and NPA

We examined potassium transport proteins and ion channels in response to low-potassium stress under different

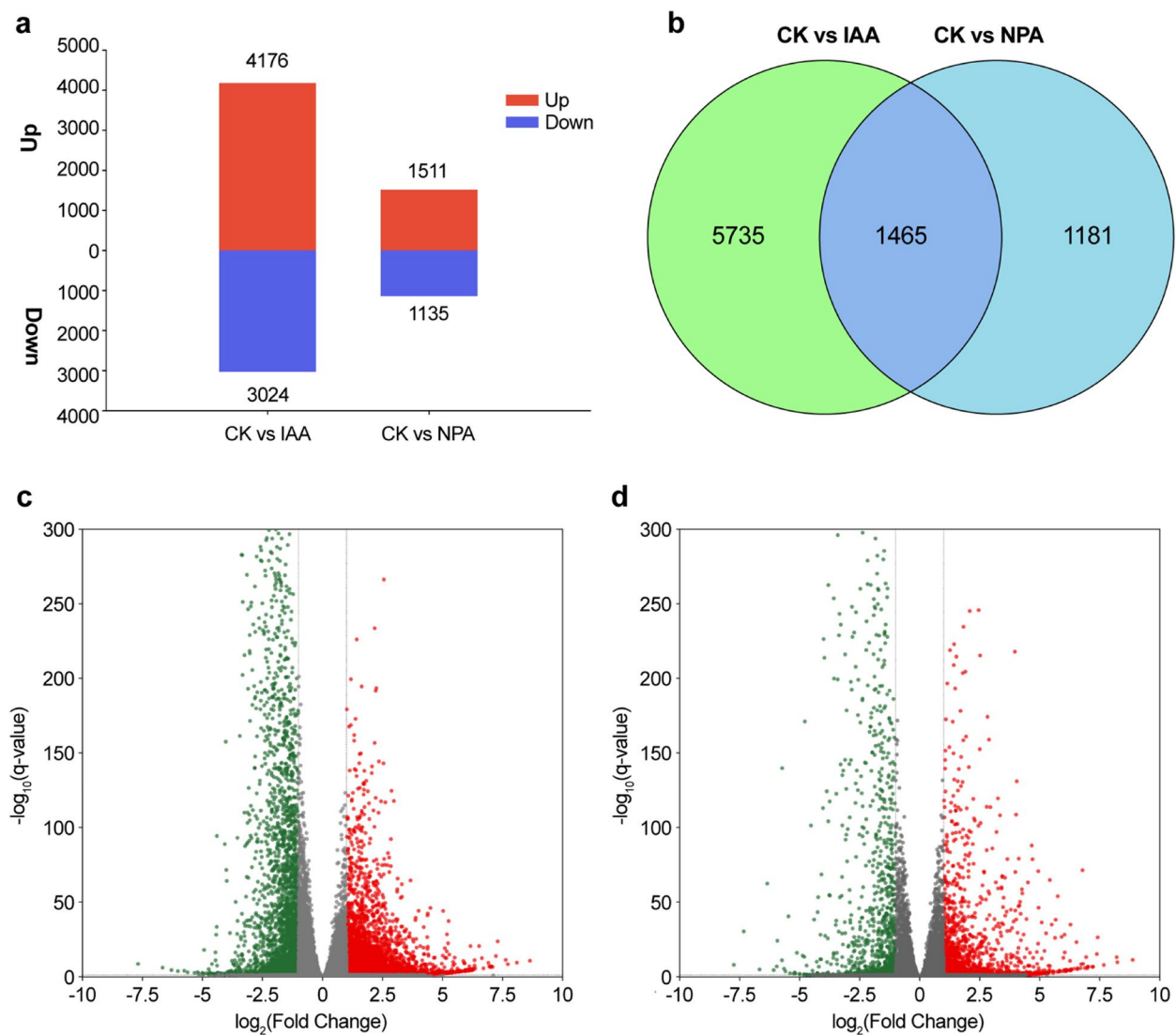


Fig. 4 Differentially expressed genes (DEG) Analysis. **a** A bar chart showing the total number of differentially upregulated (red) and downregulated (blue) genes under different treatments. **b** Venn diagram showing the shared and unique DEGs between different treatment groups. **c** and **d** Volcano plots showing the distribution of DEGs across treatment groups

treatment conditions and identified 46 DEGs. These include: (1) Shaker ion channels: *AKT1* that regulates potassium absorption, *AKT2/3* that is involved in photosynthesis-induced potassium transport in the phloem, *SKOR* that mediates K^+ release from root cortical cells to the xylem, and *NKT3* that was expressed in roots and induced by low-potassium and drought signals); (2) KUP/HAK/KT family: consists of high-affinity potassium transporters such as *HAK5*, *KUP6*, and *KUP11*; (3) HKT transporters: consist of genes such as *HKT1*; (4) TPK-type channels: mediates potassium efflux from the vacuole; (5) *CHX17*: mediates K^+ uptake and homeostasis in root cells; and (6) *KEA4*: regulates potassium absorption and chloroplast development, while is also located in chloroplasts, with six DEGs showing

changes in response to both exogenous IAA and NPA treatments (Fig. 7). These genes may be sensitive to shifts in endogenous auxin concentrations in the roots of tobacco seedlings under low-potassium stress.

Response of TF domain genes to exogenous IAA and NPA

TFs are essential regulators of nearly all plant biological processes. They influence gene transcription by binding directly or indirectly to the promoter regions of target genes. Several TF families, including AP2/ERF, MYB, NAC, WRKY, and bZIP play key roles in plant root development and potassium uptake. In this study, we have examined the expression of TF domain genes in these families following exogenous IAA and NPA treatments (Fig. 8).

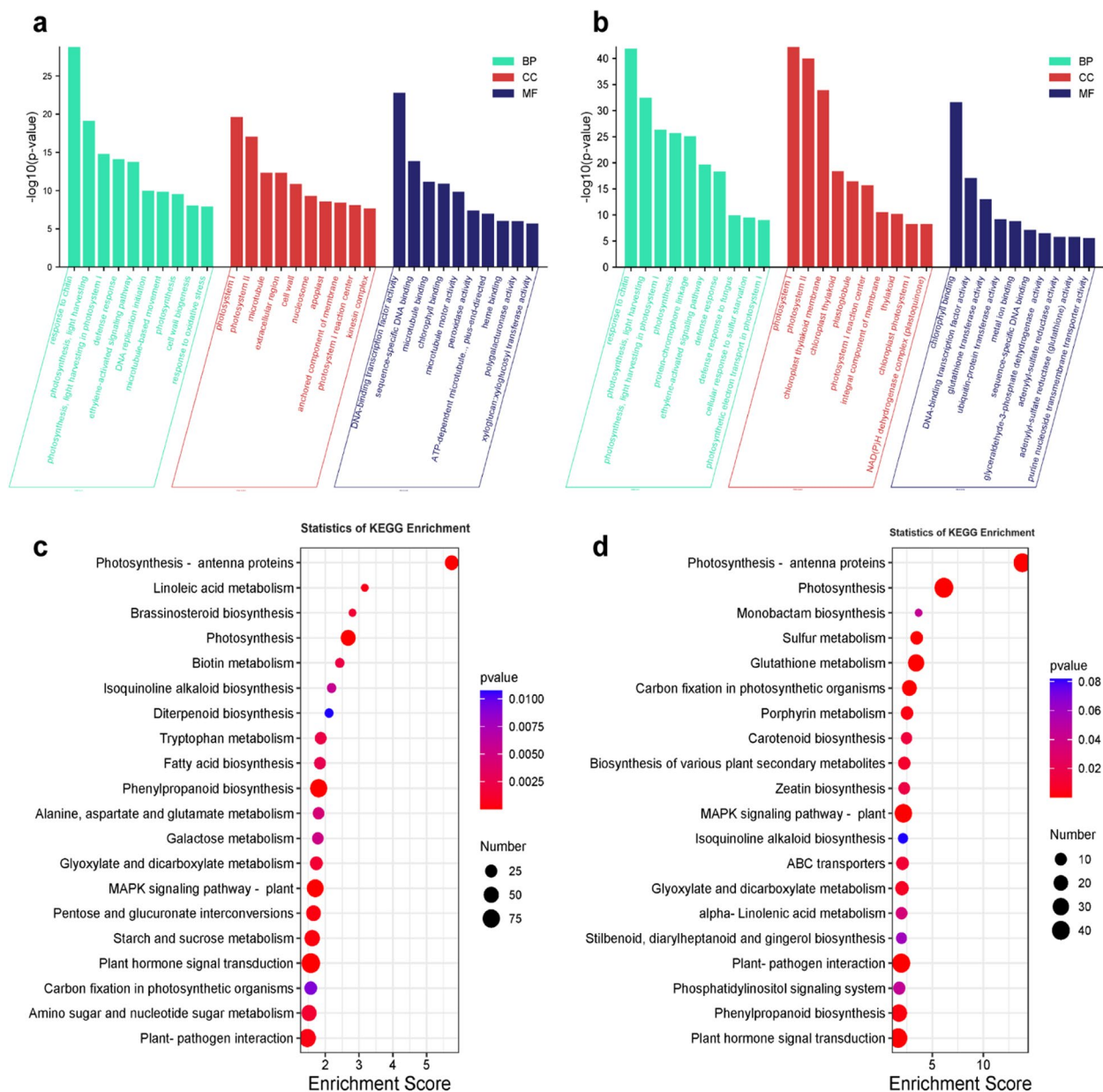


Fig. 5 GO and KEGG enrichment analysis of DEGs under low potassium conditions. **a** The top ten significant enrichment GO terms in the categories of BP, CC, and MF in the exogenous IAA-treated group. **b** The top ten significant enrichment GO terms in the categories of BP, CC, and MF in NPA treated group. **c** The top twenty significant enrichment KEGG pathways in the exogenous IAA-treated group. **d** The top twenty significant enrichment KEGG pathways in the NPA-treated group. BP: biological process; CC: cellular component; MF: molecular function

In the exogenous IAA treatment group, 194 differentially expressed TF domain genes were identified, of which 67 were upregulated and 127 were downregulated. The AP2/ERF family had the most DEGs, with 29 upregulated and 30 downregulated genes, followed by the WRKY, MYB, and NAC families. In the NPA treatment group, 99 TF domain genes were affected, with 44 upregulated and 55 downregulated genes. Compared with other families, AP2/ERFs, MYBs, and WRKYs showed greater sensitivity

to NPA treatment. Specifically, MYB was upregulated in 18 patients, whereas WRKYs and AP2/ERFs were downregulated in 21 and 20 patients, respectively.

Quantitative real-time PCR analysis

In order to validate the transcriptome data accuracy and reproducibility, six genes were randomly selected from the LK and NK treatment data for qRT-PCR analysis (Fig. 9). The results showed that the qRT-PCR data for

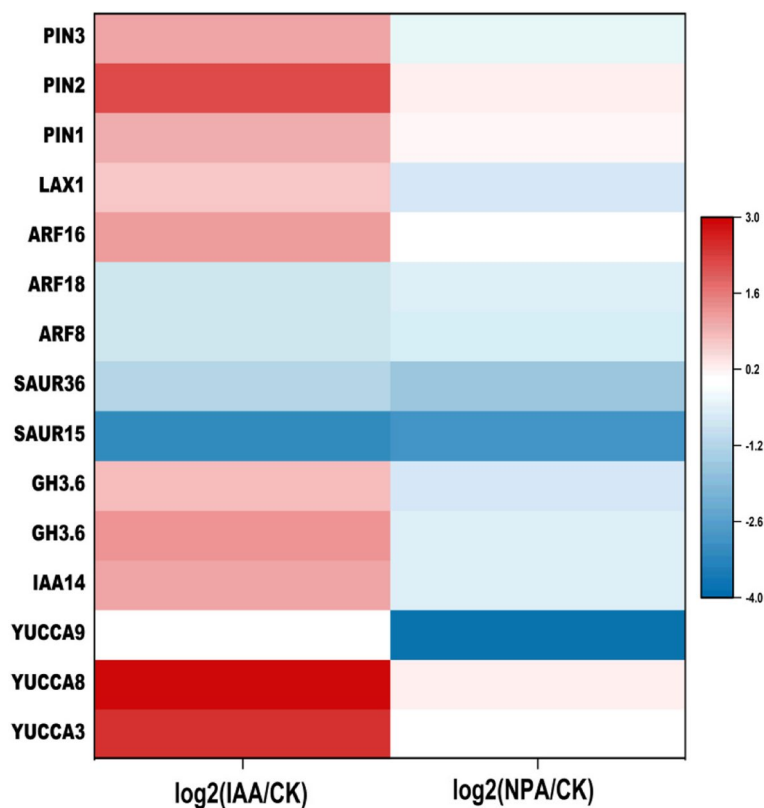


Fig. 6 Heatmap of the expression profiles of genes related to auxin biosynthesis and signal transduction. Changes in expression levels are represented by the color gradient, where red indicates high expression levels and blue indicates low expression levels

these six genes were consistent with the transcriptome sequencing results, indicating the high reliability of the transcriptome data analysis.

Discussion

Potassium deficiency stress is a common abiotic stress in field crops that affects plant growth and development at the physiological, biochemical, cellular, and molecular levels [16, 46, 47]. The root system is a crucial organ for nutrient absorption in plants, and its development and vitality are closely related to potassium absorption [48]. In the present study, we found that root dry matter accumulation under normal potassium supply was higher than that under low potassium levels, indicating that low potassium stress is detrimental to tobacco root development, which is consistent with previous findings [49].

Auxins play a pivotal role in regulating root adaptations to potassium deficiency. Under low potassium conditions, auxin signaling influences primary root growth, lateral root initiation, and root hair development [50]. In addition, auxin mitigates the inhibition of lateral root growth caused by potassium deficiency in a concentration-dependent manner [1, 20]. In our study, exogenous IAA treatment under low potassium

conditions significantly increased endogenous auxin levels in both primary and lateral root tips, suggesting that exogenous IAA alters the distribution of endogenous auxin in tobacco roots. This exogenous IAA treatment may enhance root metabolic activity by increasing the endogenous auxin content, thereby promoting root development. Notably, after application of NPA, the endogenous auxin concentration in the primary root tip decreased, whereas it significantly increased in the lateral root tip. Furthermore, NPA inhibited root development in tobacco under both normal and low-potassium conditions, suggesting that elevated endogenous auxin levels may suppress lateral root growth.

Transcriptome sequencing revealed that two key enzyme genes in the IAA biosynthesis pathway, *YUCCA3* and *YUCCA8*, were significantly upregulated following exogenous IAA treatment, whereas another enzyme gene, *YUCCA9*, was notably downregulated following NPA treatment. In addition, GH3 family genes, which indicate auxin concentration and signal strength, and changes in Aux/IAA protein levels directly reflect fluctuations in endogenous auxin levels [51]. In this study, *IAA14* was significantly upregulated and *GH3.6* downregulated following exogenous IAA and NPA treatment,

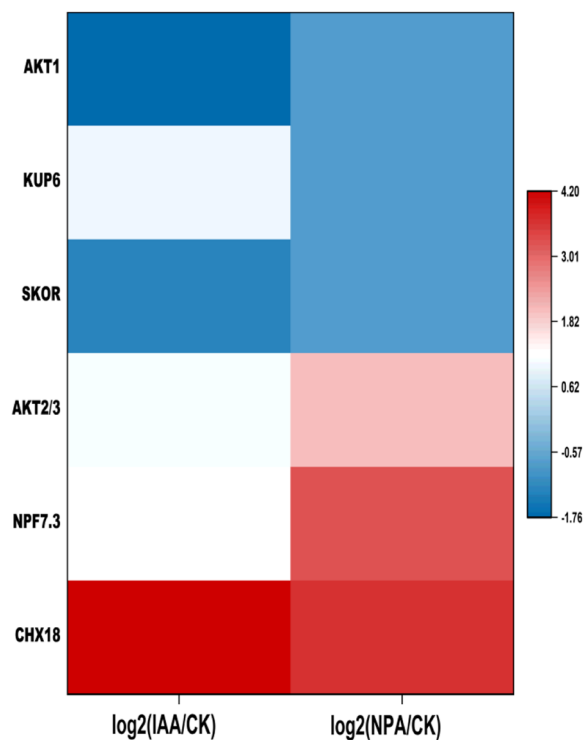


Fig. 7 Heatmap of the expression profiles of genes related to potassium ion transport channels and transport proteins. Changes in expression levels are represented by color gradient, where red indicates high expression levels and blue indicates low expression levels

respectively. These gene expression alterations are likely to contribute to the observed changes in the endogenous IAA content after treatment. Based on observed trends in root morphology, endogenous IAA levels, and key gene expression, it can be inferred that auxin regulation in tobacco root development under low potassium stress is dependent on concentration. Auxin polar transport creates an auxin concentration gradient at the root tip that is essential for root development [52]. During polar transport, the PIN family serves as the primary auxin carrier [53–55]. ARF TFs regulate auxin-responsive gene expression and influence auxin concentration in plants. In our study, under low potassium stress, *PIN1*, *PIN2*, and *PIN3* were significantly upregulated after exogenous IAA treatment, whereas *ARF8* and *ARF18* were downregulated in both treatment groups. These genes are likely to contribute to auxin distribution in tobacco, thereby regulating root development.

Exogenous auxin application enhances potassium uptake under low potassium stress [1, 56]. In this study, based on root potassium content and absorption kinetics, we observed that auxin alleviated potassium stress to some degree, whereas inhibitors reduced root potassium ion concentrations. Potassium ion flux characteristics can be used to further quantify mineral nutrient dynamics in plant roots. Interestingly, when using the patch-clamp technique to record protoplast data, we found that the EPC-9 patch-clamp could only capture the ion channel current under extremely high potassium conditions, limiting its applicability in this study. This suggests that potassium ion channels play a minimal role in the transmembrane movement of root cells under low

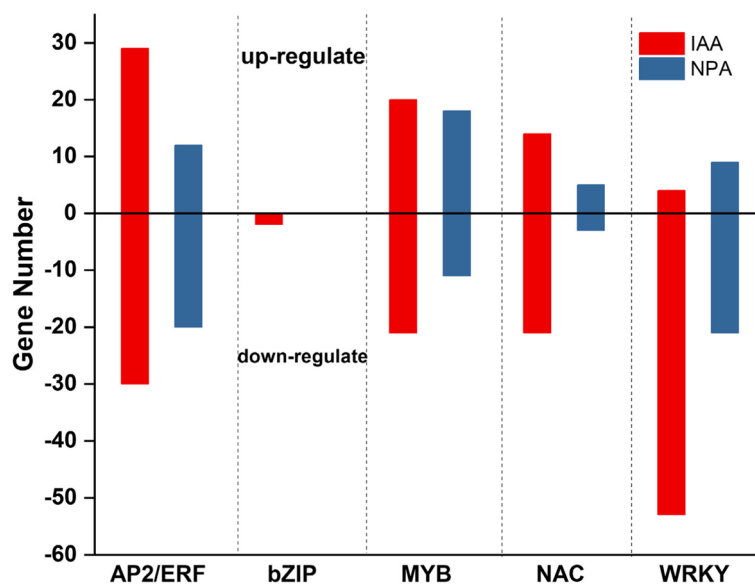


Fig. 8 Analysis of differentially expressed TF domain-containing genes of seven common TF families in the two treated groups

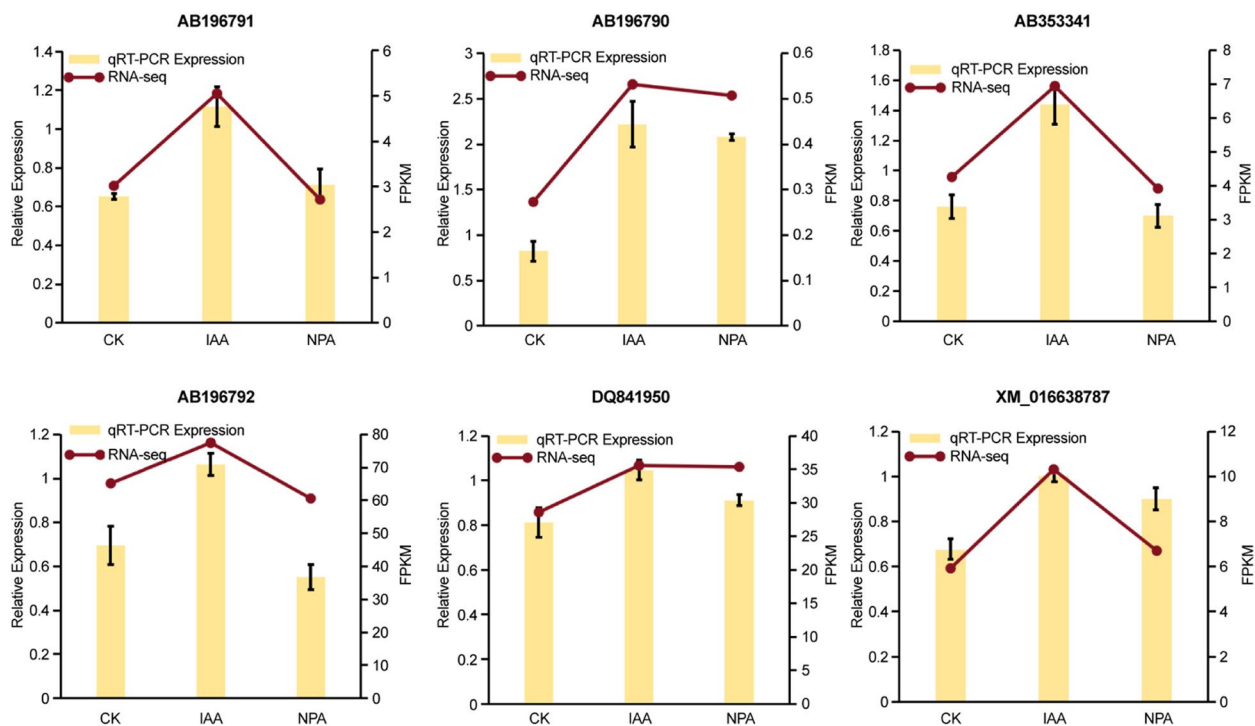


Fig. 9 The figure illustrates the validation of DEG expression patterns by qRT-PCR. The left y-axis represents the relative gene expression levels assessed by qRT-PCR, while the right y-axis displays the expression levels of selected genes calculated using the fragments per kilobase per million reads (FPKM) method. Bars represent the averages \pm SD of three replicates

potassium conditions. To address this limitation, we used NMT technology to monitor and visualize potassium ion flow and flux rates in real-time under various treatments. The results indicated that plants grown under low potassium conditions exhibited substantial potassium uptake, whereas plants grown under normal potassium conditions displayed substantial potassium excretion. After exogenous auxin application, potassium uptake in low-potassium-stressed tobacco roots increased, whereas potassium excretion in normal-potassium roots decreased, promoting potassium retention and absorption. This suggests that exogenous auxin enhances potassium absorption by roots. Conversely, after the addition of an auxin transport inhibitor, potassium uptake in low-potassium tobacco roots decreased, and potassium excretion in normal potassium roots became more pronounced, indicating that inhibitors impede potassium absorption and retention.

Potassium absorption and transport in plant roots primarily occur through potassium transporters and ion channels [26, 57–60]. *AKT1* regulates potassium-dependent root growth by modulating the degradation of *PINI* in roots and redistributing auxin [24]. *KUP9* supports root growth under low potassium stress in Arabidopsis by regulating auxin homeostasis at the root tips, thereby enhancing potassium absorption [18]. Auxin treatment

significantly increased the inward potassium ion channel genes *NKT2* and *NtKC1* expression and reduced the outward potassium ion channel gene *NtORK1* expression. These findings indicate a complex interplay between low-potassium signaling and auxin transduction. In this study, we observed that under low potassium stress, several DEGs from the HAK/KUP/KT family were present in the roots of tobacco plants treated with exogenous IAA, suggesting that exogenous IAA plays a crucial role in promoting root potassium uptake and regulating the transport of potassium from roots to shoots. Further analysis revealed that *NtKUP6* expression increased with IAA treatment and decreased with NPA treatment. The homologous gene *KUP8* in Arabidopsis is known to regulate root growth and potassium uptake, and alleviate heavy metal stress [61, 62]. We speculate that *NtKUP6* is a key gene involved in the auxin-mediated alleviation of low potassium stress in tobacco and is potentially linked to endogenous auxin concentrations, although the precise mechanism requires further investigation.

Ethylene is a key signal in plant responses to low potassium stress [63]. In this study, we discovered that DEGs in both the exogenous IAA and NPA treatments were significantly enriched in the GO term “ethylene-activated signaling pathway”. Previous research has suggested that ethylene and auxin may cooperate to regulate root

growth and development under low-potassium conditions, with ethylene acting as an upstream component of the auxin signaling pathway by regulating auxin synthesis and distribution.

TFs are ubiquitous in plants and play critical roles in activating the genes associated with abiotic stress [62]. We examined the effects of exogenous IAA and NPA on the expression of five major TF domain-containing gene families: AP2/ERF, MYB, NAC, WRKY, and bZIP. Among these, the AP2/ERF, MYB, and WRKY TFs showed the highest representation. High AP2/ERF expression under low potassium stress has been observed in rice and maize [64, 65], playing a key role in auxin-induced root development [66]. In Arabidopsis, *RAP2.11* regulates potassium ion transport by modulating AtHAK5 expression under low potassium conditions [61], whereas Lv et al. [67] demonstrated that the degradation of the auxin-induced TF ERF13 promoted lateral root formation, and MYB TFs form an essential regulatory family in plants. *MYB59* has been shown to enhance the transport of potassium ion/NO₃⁻ from roots to shoots. This is done by regulating *NRT1.5* and *NPF7.3* in Arabidopsis [68], and *SiMYB3* expression in foxtail millet, promoting primary root elongation in transgenic Arabidopsis, and improving tolerance to potassium deficiency [69]. The WRKY TF family plays a role in plant defense responses [70]. *WRKY6* regulates root potassium ion absorption in Arabidopsis by promoting *AKT1* [71]. In this study, we identified candidate genes that may help elucidate the molecular mechanisms of auxin-regulated tobacco root development under low-potassium stress. Whether these differentially expressed auxin-responsive TFs are directly involved in potassium ion absorption remains an area of further investigation.

Conclusion

Potassium deficiency impairs root development and uptake, and the response of tobacco roots to potassium deficiency is closely linked to the endogenous auxin concentration. Transcriptome sequencing revealed that DEGs are predominantly enriched in metabolic pathways, including photosynthesis, antenna proteins, plant hormone signal transduction, and the MAPK signaling pathway in plants. Analysis of DEGs related to auxin signaling, potassium ion channels and transporters, and TFs identified several key genes responsive to potassium deficiency, including *KUP6*, *IAA14*, *ARF16*, *PIN1*, *SKOR*, *NPF7.3*, and *AP2/ERF*. Notably, *KUP6* expression increased with IAA treatment and decreased with NPA treatment, indicating its critical role in auxin-mediated alleviation of potassium deficiency stress in tobacco and its association with endogenous auxin

levels. This study was conducted under hydroponic conditions, which may not fully mimic the complexity of natural soil environments. Future research should investigate a broader spectrum of potassium deficiency levels and incorporate soil-based systems to provide a more comprehensive understanding. Additionally, mechanistic studies are needed to explore the molecular interactions between auxin signaling and potassium transporters under low-potassium stress. Specifically, further investigations should focus on how key genes, such as *KUP6*, *IAA14*, and *ARF16*, regulate potassium uptake at both the cellular and molecular levels. These studies will contribute to a deeper understanding of the auxin-mediated mechanisms that alleviate stress under potassium deficiency.

Abbreviations

| | |
|------|---|
| NPA | N-1-naphthylphthalamic acid |
| DEG | Differentially expressed gene |
| ARF | Auxin response factor |
| NMT | Non-invasive micro-test technology |
| GO | Gene Ontology |
| KEGG | Kyoto Encyclopedia of Genes and Genomes |
| PCA | Principal component analysis |
| TFs | Transcription factors |

Acknowledgements

The authors thank Can Liu and Yabin Hou for their valuable suggestions on data analysis and discussion. We also thank Guo Ze for his assistance with the experiments.

Authors' contributions

KH.G conducted the experiments, analyzed the data, and wrote the manuscript. L and Z assisted with the experiments. D designed the study. Y.Z.Y.G, and D reviewed and revised the manuscript. All authors read and approved the final manuscript.

Funding

This study was funded by a grant from the National Natural Science Foundation of China (No. 31501823) and the Henan Provincial Science and Technology Research Project, China (No. 25210211122).

Data availability

The sequencing data supporting the findings of this study are available in the NCBI Sequence Read Archive (SRA) under the accession number SRP543827.

Declarations

Ethics approval and consent to participate

Not applicable.

Consent for publication

Not applicable.

Competing interests

The authors declare no competing interests.

Author details

¹College of Tobacco Science, Henan Agricultural University, Key Laboratory for Tobacco Cultivation in Tobacco Industry, Zhengzhou 450002, China.

Received: 11 October 2024 Accepted: 22 April 2025

Published online: 19 May 2025

References

- Song W, Liu S, Meng L, Xue R, Wang C, Liu G, Dong C, Wang S, Dong J, Zhang YJP, et al. Potassium deficiency inhibits lateral root development in tobacco seedlings by changing auxin distribution. *Plant and Soil*. 2015;396:163–73.
- Wang M, Zheng Q, Shen Q, Guo S. The Critical Role of Potassium in Plant Stress Response. *Int J Mol Sci*. 2013;14(4):7370–90.
- Mondy N, Mobley EO, Gedde-Dahl SB. Influence of potassium fertilization on enzymatic activity, phenolic content and discoloration of potatoes. *J Food Sci*. 1967;32(4):378–81.
- Mengel K, Arneke WW. Effect of potassium on the water potential, the pressure potential, the osmotic potential and cell elongation in leaves of *Phaseolus vulgaris*. *Physiologia plantarum*. 1982;54(4):402–8.
- Zhao D, Oosterhuis DM, Bednarz CW. Influence of potassium deficiency on photosynthesis, chlorophyll content, and chloroplast ultrastructure of cotton plants. *Photosynthetica*. 2001;39:103–9.
- Zeng Q, Ling Q, Fan L, Li Y, Hu F, Chen J, Huang Z, Deng H, Li Q, Qi YJPO. Transcriptome profiling of sugarcane roots in response to low potassium stress. *PLoS one*. 2015;10(5):e0126306.
- Bilias F, Kalderis D, Richardson C, Barbayiannis N, Gasparatos D. Biochar application as a soil potassium management strategy: A review. *Sci Total Environ*. 2023;858:159782.
- Samal D, Kovar JL, Steingrobe B, Sadana US, Bhadoria PS, Claassen N. Soil: Potassium uptake efficiency and dynamics in the rhizosphere of maize (*Zea mays* L.), wheat (*Triticum aestivum* L.), and sugar beet (*Beta vulgaris* L.) evaluated with a mechanistic model. *Plant and Soil*. 2010;332:105–21.
- Chen G, Feng H, Hu Q, Qu H, Chen A, Yu L, Xu G. Improving rice tolerance to potassium deficiency by enhancing Os HAK 16p: WOX 11-controlled root development. *Plant Biotechnol J*. 2015;13(6):833–48.
- Han M, Wu W, Wu W-H, Wang Y. Potassium transporter KUP7 is involved in K⁺ acquisition and translocation in Arabidopsis root under K⁺-limited conditions. *Mol Plant*. 2016;9(3):437–46.
- Li W, Xu G, Alli A, Yu L. Plant HAK/KUP/KT K⁺ transporters: function and regulation. *Semin Cell Dev Biol*. 2018;74:133–41.
- Chen J, Gabelman WH. Morphological and physiological characteristics of tomato roots associated with potassium-acquisition efficiency. *Sci Hortic*. 2000;83(3–4):213–25.
- Kellermeier F, Chardon F, Amtmann AJPP. Natural variation of Arabidopsis root architecture reveals complementing adaptive strategies to potassium starvation. *Plant Physiol*. 2013;161(3):1421–32.
- Zhao X-H, Yu HQ, Jing W, Wang X-G, Qi D, Jing W, Qiao WJ. Response of root morphology, physiology and endogenous hormones in maize (*Zea mays* L.) to potassium deficiency. *Plant J*. 2016;15(4):785–94.
- Guo Z, Li Z-S, Dai X-Y, Wang Y-F. Fertilizers: Effects of auxin on tobacco root growth and potassium uptake under low potassium stress. *J Plant Nutr Fertilizers*. 2019;25(7):1173–84.
- Zeng J, Quan X, He X, Cai S, Ye Z, Chen G, Zhang G. Root and leaf metabolite profiles analysis reveals the adaptive strategies to low potassium stress in barley. *BMC Plant Biol*. 2018;18:1–13.
- Huang L, Jiang Q, Wu J, An L, Zhou Z, Wong C, Wu M, Yu H, Gan Y. Zinc finger protein 5 (ZFP5) associates with ethylene signaling to regulate the phosphate and potassium deficiency-induced root hair development in Arabidopsis. *Plant Mol Biol*. 2020;102:143–58.
- Zhang ML, Huang PP, Ji Y, Wang S, Wang SS, Li Z, Guo Y, Ding Z, Wu WH, Wang Y. KUP 9 maintains root meristem activity by regulating K⁺ and auxin homeostasis in response to low K. *EMBO Rep*. 2020;21(6):e50164.
- Woodward AW, Bartel B. Auxin: regulation, action, and interaction. *Ann Bot*. 2005;95(5):707–35.
- Zhang S, Qiu L, Zheng Y, Wang W, Zhao H, Yang D. Comparative transcriptome analysis reveals the regulatory effects of exogenous auxin on lateral root development and tanshinone accumulation in *Salvia miltiorrhiza*. *Planta*. 2023;258(2):33.
- Ma T-L, Wu W-H, Wang Y. Transcriptome analysis of rice root responses to potassium deficiency. *BMC Plant Biol*. 2012;12:1–13.
- Ruan L, Zhang J, Xin X, Zhang C, Ma D, Chen L, Zhao B. Comparative analysis of potassium deficiency-responsive transcriptomes in low potassium susceptible and tolerant wheat (*Triticum aestivum* L.). *Sci Rep*. 2015;5(1):10090.
- Xiong W, Wang Y, Guo Y, Tang W, Zhao Y, Yang G, Pei Y, Chen J, Song X, Sun J. Transcriptional and metabolic responses of maize shoots to long-term potassium deficiency. *Front Plant Sci*. 2022;13:922581.
- Li J, Wu WH, Wang Y. Potassium channel AKT1 is involved in the auxin-mediated root growth inhibition in Arabidopsis response to low K⁺ stress. *J Integr Plant Biol*. 2017;59(12):895–909.
- Vicente-Agullo F, Rigas S, Desbrosses G, Dolan L, Hatzopoulos P, Grabov A. Potassium carrier TRH1 is required for auxin transport in Arabidopsis roots. *Plant J*. 2004;40(4):523–35.
- Zhao S, Zhang M-L, Ma T-L, Wang Y. Phosphorylation of ARF2 relieves its repression of transcription of the K⁺ transporter gene HAK5 in response to low potassium stress. *Plant Cell*. 2016;28(12):3005–19.
- Muday GK, Rahman A, Binder BM. Auxin and ethylene: collaborators or competitors? *Trends Plant Sci*. 2012;17(4):181–95.
- Shen H, Chen J, Wang Z, Yang C, Sasaki T, Yamamoto Y, Matsumoto H, Yan X. Root plasma membrane H⁺-ATPase is involved in the adaptation of soybean to phosphorus starvation. *J Exp Bot*. 2006;57(6):1353–62.
- Gong Q, Li Z, Wang L, Dai T, Kang Q, Niu D. Exogenous of indole-3-acetic acid application alleviates copper toxicity in spinach seedlings by enhancing antioxidant systems and nitrogen metabolism. *Toxics*. 2019;8(1):1.
- Khalid A, Aftab F. Biology-Plant D: Effect of exogenous application of IAA and GA 3 on growth, protein content, and antioxidant enzymes of *Solanum tuberosum* L. grown in vitro under salt stress. *In vitro Cell Dev Biol-Plant*. 2020;56:377–89.
- Zhang Y, Li Y, Hassan MJ, Li Z, Peng Y. Indole-3-acetic acid improves drought tolerance of white clover via activating auxin, abscisic acid and jasmonic acid related genes and inhibiting senescence genes. *BMC Plant Biol*. 2020;20:1–12.
- Abas L, Kolb M, Stadlmann J, Janacek DP, Lukic K, Schwechheimer C, Sazanov LA, Mach L, Friml J, Hammes UZ. Naphthylphthalamic acid associates with and inhibits PIN auxin transporters. *Proc Natl Acad Sci USA*. 2021;118(1):e2020857118.
- Wang Y, Dai X, Xu G, Dai Z, Chen P, Zhang T, Zhang H. The Ca²⁺-CaM signaling pathway mediates potassium uptake by regulating reactive oxygen species homeostasis in tobacco roots under low-K⁺ stress. *Front Plant Sci*. 2021;12:658609.
- Hu W, Di Q, Wang Z, Zhang Y, Zhang J, Liu J, Shi X. Grafting alleviates potassium stress and improves growth in tobacco. *BMC Plant Biol*. 2019;19:1–13.
- Comas LH, Eissenstat DM, Lakso AN. Assessing root death and root system dynamics in a study of grape canopy pruning. *New Phytol*. 2000;147(1):171–8.
- Hochholdinger F, Woll K, Guo L, Schnable PS. The accumulation of abundant soluble proteins changes early in the development of the primary roots of maize (*Zea mays* L.). *Proteomics*. 2005;5(18):4885–93.
- Fan L, Zhou W, Shang S, Zhou S, Gao S, Shaaban M, Wang Z, Shi G. Deciphering the auxin-ethylene crosstalk in petal abscission through auxin influx carrier IpAUX1 of *Itoh peony* 'Bartzella'. *Postharvest Biol and Technol*. 2024;216:113060.
- Li Y, Feng Y, Zhao Y, Ma Y, Liu D, Shi H. Effects of nitrogen forms on absorption kinetics and transcriptome of flue-cured tobacco and burley tobacco. *Acta Tabacaria Sinica*. 2023;29(6):52–63.
- Liang T, Dai H, Khan WA, Guo Y, Meng X, Wang G, Zhang Y. Topping Inhibited Potassium Uptake via Regulating Potassium Flux and Channel Gene Expression in Tobacco. *Agronomy*. 2022;12(5):1166.
- Chen S, Zhou Y, Chen Y, Gu J. fastp: an ultra-fast all-in-one FASTQ preprocessor. *Bioinformatics*. 2018;34(17):i884–90.
- Kim D, Langmead B, Salzberg SL. HISAT: a fast spliced aligner with low memory requirements. *Nat Methods*. 2015;12(4):357–60.
- Roberts A, Trapnell C, Donaghey J, Rinn JL, Pachter L. Improving RNA-Seq expression estimates by correcting for fragment bias. *Genome Biol*. 2011;12:1–14.
- Anders S, Pyl PT, Huber W. HTSeq—a Python framework to work with high-throughput sequencing data. *Bioinformatics*. 2015;31(2):166–9.
- Research GOC. The gene ontology resource: 20 years and still GOing strong. *Nucleic Acids Res*. 2019;47(D1):D330–8.
- Kanehisa M, Araki M, Goto S, Hattori M, Hirakawa M, Itoh M, Katayama T, Kawashima S, Okuda S, Tokimatsu T. KEGG for linking genomes to life and the environment. *Nucleic Acids Res*. 2007;36(suppl_1):D480–4.
- Ashley M, Grant M, Grabov A. Plant responses to potassium deficiencies: a role for potassium transport proteins. *J Exp Bot*. 2006;57(2):425–36.
- Britto DT, Kronzucker HJ. Cellular mechanisms of potassium transport in plants. *Physiol Plant*. 2008;133(4):637–50.

48. Maathuis FJ, Sanders D. Mechanisms of potassium absorption by higher plant roots. *Physiol Plantarum*. 1996;96(1):158–68.
49. Song W, Xue R, Song Y, Bi Y, Liang Z, Meng L, Dong C, Wang C, Liu G, Dong J. Differential response of first-order lateral root elongation to low potassium involves nitric oxide in two tobacco cultivars. *J Plant Growth Reg*. 2018;37:114–27.
50. Overvoorde P, Fukaki H, Beeckman T. Auxin control of root development. *Cold Spring Harb Perspect Biol*. 2010;2(6):a001537.
51. Yu Z, Zhang F, Friml J, Ding Z. Auxin signaling: Research advances over the past 30 years. *J Integr Plant Biol*. 2022;64(2):371–92.
52. Da-Xi Z, Ke Y, Zhi-Hong X, Hong-Wei XU. Effect of polar auxin transport on rice root development. *J Integr Plant Biol*. 2003;45(12):1421.
53. Petrášek J, Mravec J, Bouchard R, Blakeslee JJ, Abas M, Seifertová D, Wisniewska J, Tadele Z, Kubes M, Covanová M. PIN proteins perform a rate-limiting function in cellular auxin efflux. *Science*. 2006;312(5775):914–8.
54. Adamowski M, Friml J. PIN-dependent auxin transport: action, regulation, and evolution. *Plant Cell*. 2015;27(1):20–32.
55. Ung KL, Winkler M, Schulz L, Kolb M, Janacek DP, Dedec E, Stokes DL, Hammes UZ, Pedersen BP. Structures and mechanism of the plant PIN-FORMED auxin transporter. *Nature*. 2022;609(7927):605–10.
56. Zhou D, Zhang Y, Dong Q, Wang K, Zhang H, Du Q, Wang J, Wang X, Yu H, Zhao X. Integrated Transcriptomic and Metabolomic Analysis of Exogenous NAA Effects on Maize Seedling Root Systems under Potassium Deficiency. *Int J Mol Sci*. 2024;25(6):3366.
57. Ahn SJ, Shin R, Schachtman DP. Expression of KT/KUP genes in Arabidopsis and the role of root hairs in K⁺ uptake. *Plant Physiol*. 2004;134(3):1135–45.
58. Yang T, Zhang S, Hu Y, Wu F, Hu Q, Chen G, Cai J, Wu T, Moran N, Yu L. The role of a potassium transporter OsHAK5 in potassium acquisition and transport from roots to shoots in rice at low potassium supply levels. *Plant Physiol*. 2014;166(2):945–59.
59. Shen Y, Shen L, Shen Z, Jing W, Ge H, Zhao J, Zhang W. The potassium transporter Os HAK 21 functions in the maintenance of ion homeostasis and tolerance to salt stress in rice. *Plant Cell Environ*. 2015;38(12):2766–79.
60. Cai K, Zeng F, Wang J, Zhang G. Identification and characterization of HAK/KUP/KT potassium transporter gene family in barley and their expression under abiotic stress. *BMC Genomics*. 2021;22(1):317.
61. Osakabe Y, Arinaga N, Umezawa T, Katsura S, Nagamachi K, Tanaka H, Ohiraki H, Yamada K, Seo S-U, Abo M. Osmotic stress responses and plant growth controlled by potassium transporters in Arabidopsis. *Plant Cell*. 2013;25(2):609–24.
62. Sanz-Fernández M, Rodríguez-González A, Sandalio LM, Romero-Puertas MC. Role of potassium transporter KUP8 in plant responses to heavy metals. *Physiol Plant*. 2021;173(1):180–90.
63. Hayashi K-I. The interaction and integration of auxin signaling components. *Plant Cell Physiol*. 2012;53(6):965–75.
64. Zhang X, Jiang H, Wang H, Cui J, Wang J, Hu J, Guo L, Qian Q, Xue D. Transcriptome analysis of rice seedling roots in response to potassium deficiency. *Sci Rep*. 2017;7(1):5523.
65. Guo S, Liu Z, Sheng H, Olukayode T, Zhou Z, Liu Y, Wang M, He M, Kochian L, Qin Y. Dynamic transcriptome analysis unravels key regulatory genes of maize root growth and development in response to potassium deficiency. *Planta*. 2023;258(5):99.
66. Nie J, Wen C, Xi L, Lv S, Zhao Q, Kou Y, Ma N, Zhao L, Zhou X. The AP2/ERF transcription factor CmERF053 of chrysanthemum positively regulates shoot branching, lateral root, and drought tolerance. *Plant Cell Rep*. 2018;37:1049–60.
67. Lv B, Wei K, Hu K, Tian T, Zhang F, Yu Z, Zhang D, Su Y, Sang Y, Zhang X. MPK14-mediated auxin signaling controls lateral root development via ERF13-regulated very-long-chain fatty acid biosynthesis. *Mol Plant*. 2021;14(2):285–97.
68. Du X-Q, Wang F-L, Li H, Jing S, Yu M, Li J, Wu W-H, Kudla J, Wang Y. The transcription factor MYB59 regulates K⁺/NO₃⁻ translocation in the Arabidopsis response to low K⁺ stress. *Plant Cell*. 2019;31(3):699–714.
69. Cao X, Hu L, Chen X, Zhang R, Cheng D, Li H, Xu Z, Li L, Zhou Y, Liu A. Genome-wide analysis and identification of the low potassium stress responsive gene SiMYB3 in foxtail millet (*Setaria italica* L.). *BMC Genomics*. 2019;20:1–13.
70. Rushton PJ, Somssich IE, Ringler P, Shen QJ. WRKY transcription factors. *Trends Plant Sci*. 2010;15(5):247–58.
71. Niu F, Cui X, Yang B, Wang R, Zhao P, Zhao X, Zhang H, Fan X, Li Y, Deyholos MK. WRKY6 transcription factor modulates root potassium acquisition through promoting expression of AKT1 in Arabidopsis. *Plant J*. 2024;118(5):1652–67.

Publisher's Note

Springer Nature remains neutral with regard to jurisdictional claims in published maps and institutional affiliations.